Dating emplacement and evolution of the orogenic magmatism in the internal Western Alps: 1. The Miagliano Pluton

**Alfons Berger · Tonny B. Thomsen ·
Maria Ovtcharova · Notburga Kapferer ·
Ivan Mercolli**

Abstract The Canavese Line in the Western Alps represents the position in the Alpine chain, where alkaline and calc-alkaline magmatism occur in close spatial and temporal association. In addition to available data on the alkaline Valle del Cervo Pluton, we present petrological and geochemical data on the Miagliano tonalite. The latter is of special interest, because it is located in the southeastern side of the Canavese Line, in contrast to most Periadriatic Plutons. The dioritic to tonalitic rocks of the Miagliano Pluton represent an intermediate stage of a calc-alkaline differentiation, demonstrated by relics of two different pyroxenes as well as the texture of allanite. Hornblende barometry indicates pressures of $\sim$0.46 GPa consistent with the presence of magmatic epidote. Field relationships between the two Plutons, the volcanic and volcaniclastic rocks of the Biella Volcanic Suite and numerous dykes cross-cutting the different units, allow reconstruction of a more refined chronology of the calc-alkaline and alkaline magmatic series. High precision zircon geochronology yields an age of 33.00 ± 0.04 Ma for the central tonalitic part of the Miagliano Pluton and 30.39 ± 0.50 Ma for the granitic core of the Valle del Cervo Pluton. The difference in age combined with cooling data and intrusion depth indicates dissimilar tectonic transport east and west of the Canavese Line. The earlier emplaced Miagliano Pluton has to be exhumed from an intrusion depth of $\sim$12–15 km, whereas the neighbouring and younger Valle del Cervo Pluton is exhumed from a depth of 5–7 km. This tectonic scenario is related to upper crustal rigid block rotation responsible for the burial of the lowermost Rupelian paleosurface of the Sesia–Lanzo Zone. Thus, the new ages constrain the paroxysm of the orogenic magmatism in the internal Western Alps to an extremely short lapse of time in the first half of the Rupelian.

Keywords Miagliano Pluton · Isotope dating · Alkaline and calc-alkaline magmatism · Western Alps

A. Berger (✉)
Department of Geography and Geology,
University of Copenhagen, Øster Voldgade 10,
1350 Copenhagen, Denmark
e-mail: ab@geo.ku.dk

T. B. Thomsen
Department of Geological Sciences, Stockholm University,
Svante Arrhenius väg 8, 10691 Stockholm, Sweden

M. Ovtcharova
Section of Earth and Environmental Sciences,
University of Geneva, Rue de Maraîchers 13,
1205 Geneva, Switzerland

N. Kapferer · I. Mercolli
Institute of Geological Sciences, University of Bern,
Baltzerstrasse 1+3, 3012 Bern, Switzerland

1 Introduction and geological setting

The Western Alps are characterized by oceanic and continental units, which are stacked by north-westward orogenic transport as a consequence of a south-eastward directed subduction. The subduction and related imbrications occur from the late Cretaceous in the Sesia Zone to the Oligocene in the Valais units (summary in Berger and Bousquet 2008). During the subduction of the Piemont–Liguria oceanic units, the Sesia–Lanzo Zone was the hanging plate of this process. Magmatism in the Western Alps is concentrated in the vicinity of the Canavese Line, a major tectonic Lineament in the Alps (Fig. 1). The Tertiary
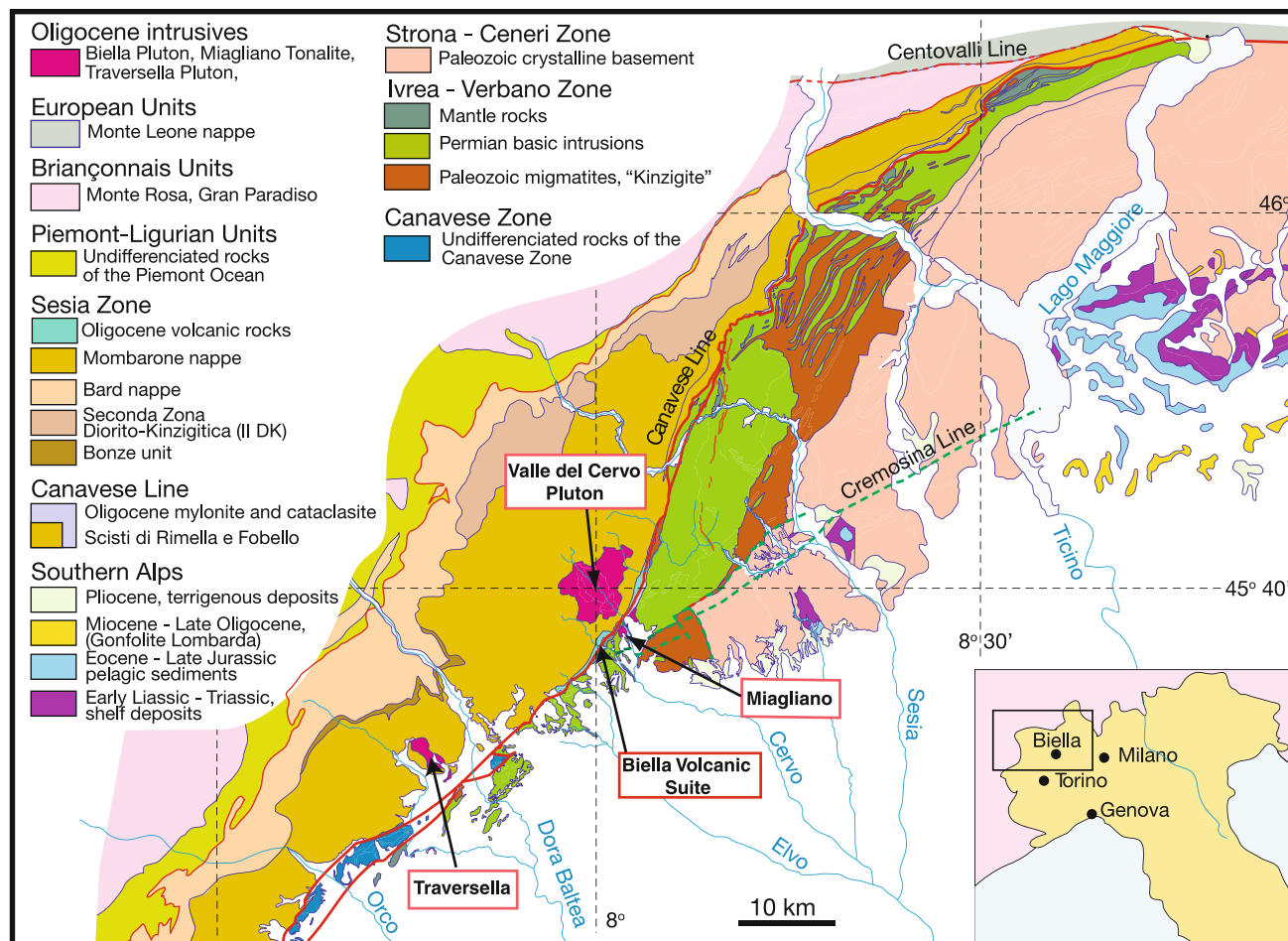
Fig. 1 Geological map of the studied area compiled after Malaroda et al. (1966); Bigi et al. (1990) and Babist et al. (2006)

orogenic magmatism in the Alps has been summarized and discussed from different points of view (e.g., von Blankenburg et al. 1998; Bonin 2004; Rosenberg 2004; Lustrino et al. 2010). Thus, here we briefly summarize the main characteristics of the magmatic rocks of interest for the present work occurring in the internal Western Alps. Further details about the source of the magmas, their fractionation and emplacement, are found in the above-mentioned reviews.

The western Alpine magmatic province includes alkaline, ultrapotassic and calc-alkaline rocks intruding an active orogen (Dal Piaz et al. 1979; Bigioggero et al. 1981, 1994; Beccaluva et al. 1983; Venturelli et al. 1984; Peccerillo and Martinotti 2006; Owen 2008; Prelević et al. 2008; Conticelli et al. 2009; Tommasini et al. 2011). In addition to widespread dykes of different magmatic affinity intruding the internal units (i.e., Piemont–Liguria, Sesia–Lanzo and Ivrea–Verbano), three Plutons are exposed: the Traversella-, Miagliano- and Valle del Cervo-Pluton (Fig. 1). The Traversella and Valle del Cervo Plutons intrude high pressure (HP) rocks of the Mombarone nappe

in the Sesia–Lanzo Zone west of the Canavese Line, whereas the Miagliano tonalite is situated in the Ivrea–Verbano Zone east of the Canavese Line (Fig. 1). The Traversella and Miagliano Plutons are typical calc-alkaline suites (Van Marcke de Lumen and Vander Auwera 1990; Carraro and Ferrara 1968) whereas the Valle del Cervo Pluton ranges in composition from monzonite to granite with a clear alkaline affinity (Bigioggero et al. 1994). The dykes show a large spread in composition (Fig. 2) from calc-alkaline, shoshonitic to ultrapotassic (lamprophyre and lamproite; Dal Piaz et al. 1979; Venturelli et al. 1984; Bellini et al. 1993; Peccerillo and Martinotti 2006; Owen 2008; Prelević et al. 2008; Conticelli et al. 2009). Subaerial volcanic rocks (Callegari et al. 2004; Kapferer et al. 2012b) cover a thin band of ca. 20 km on top of the Mombarone nappe (Sesia–Lanzo Zone) along the Canavese Line. These volcanics, summarized as the Biella Volcanic Suite (BVS on Fig. 1), also show compositional variations from calc-alkaline to shoshonitic (Figs. 1, 2; De Capitani et al. 1979; Venturelli et al. 1984; Callegari et al. 2004). Callegari et al. (2004) mapped the spatial distribution of the different types
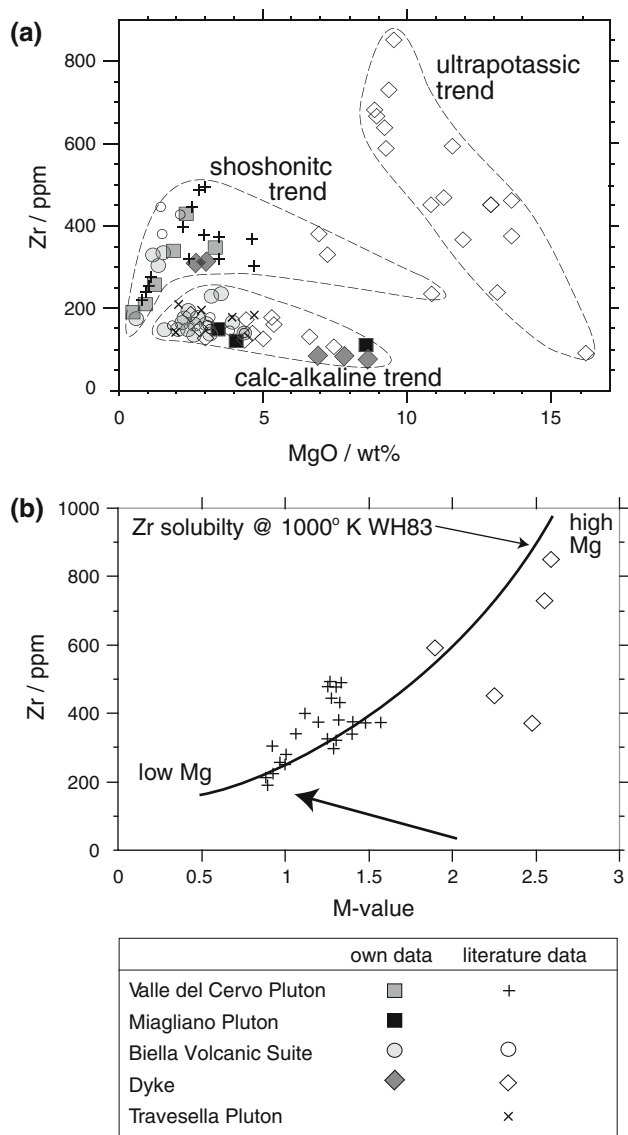
Fig. 2 Evolution of Zr in the different magmatic systems. **a** Zr versus MgO diagram. Data source in addition to own data: Venturelli et al. (1984); Bigioggero et al. (1994); Callegari et al. (2004); Owen (2008); Conticelli et al. (2009). **b** Zr versus M-value [M = (K + Na + 2 × Ca)/Al × Si]. In addition the Zr solubility calculated with the equation of Watson and Harrison (1983) is shown. *Bold arrow* in the lower part indicate general, calc-alkaline evolutions

of volcanic rocks. Thus, the preserved magmatic activity in the Western Alps comprises plutonic, subvolcanic and subaerial volcanic rocks. In addition, the magmatic rocks also differ in chemical and petrological evolution. We have combined field, petrographic and petrological observations with isotope dating (U/Pb of zircon) to constrain time and depth of emplacement of the Miagliano Pluton, its cooling and exhumation history and its relation to the magmatic and tectonic evolution of the entire area. Combining field relationships and geochemical affinity of the dykes with the known temporal evolution of the Biella Volcanic Suite,

Valle del Cervo Pluton and Miagliano Pluton, we will present a relative chronology for the dyke emplacement.

2 Sample preparation and analytical methods

Fragmentation of the rock samples into separate mineral grains was carried out at the University of Bern, Switzerland, by electro-dynamic disaggregation, employing a high voltage pulse generator (e.g., Giese et al. 2010). The fragmented material was subsequently sorted through size-proportion sieving, Franz electromagnetic separators, Wilfley shaking table concentrator and density separation using heavy liquid protocols. Separates were then mounted in epoxy or on small glass plates and polished prior to analysis.

High precision TIMS ages were obtained from single zircon grains at the Department of Mineralogy of the University of Geneva, using the equipment and following the analytical protocol for U–Pb age determinations described in detail in accompanied contribution (Kapferer et al. 2012a). Uncertainty ellipses of individual analyses are 2σ. Before TIMS analysing the zircons where characterized by cathodoluminiscence methods using a Zeiss Evo 50 SEM equipped with a Gatan Mono CL 3 device at the Institute of Geological Sciences of the University of Bern.

Bulk rock analyses were carried out by standard X-ray fluorescence (XRF) techniques on glass pellets at the Department of Geosciences of the University of Fribourg. Electron microprobe analyses was carried out on mineral separates and thin sections by a JEOL JXA8200 at the Institute of Geological Sciences of the University of Bern, using silicate and oxide standards, a beam current of 10 or 20 nA and acceleration voltages of 15 kV for rock forming silicate minerals and 25 kV for the allanite. To avoid electron beam damage from a fully focused beam, beam diameters of 5 or 10 μm was applied to most phases (for details of the allanite measurements see Janots et al. 2008).

3 Results

3.1 Field relations, petrography and mineral chemistry of the Miagliano Pluton

The Miagliano Pluton (Fig. 1) was first described by Bortolami et al. (1965) and was assigned to the tertiary magmatism by Carraro and Ferrara (1968). The Pluton is poorly outcropping, and the best outcrops can been visited along the river Cervo near the village of Miagliano. The present day total surface area of the Pluton hardly exceeds 4 km^2 (Carraro and Ferrara 1968), and includes a more or less concentric structure with a fine-grained monzodiorite

Table 1 Representative whole-rock XRF analysis of the Miagliano Pluton

Sample	Bi0431	Bi0432	Bi0637
(wt%)			
SiO_2	50.18	51.51	53.12
TiO_2	1.54	1.05	0.95
Al_2O_3	15.55	20.72	20.55
Fe_2O_3	10.42	8.70	8.10
MnO	0.16	0.15	0.16
MgO	8.57	4.06	3.45
CaO	9.22	8.47	7.71
Na_2O	2.47	2.98	3.87
K_2O	1.77	1.83	1.09
P_2O_5	0.16	0.31	0.28
L.O.I.	0.96	1.22	1.04
Sum	101.22	101.23	100.53
(ppm)			
Rb	46	58	26
Sr	399	729	701
Ba	935	802	653
Cr	<5	<5	9
Ni	10	<5	<5
Y	43	22	27
Zr	109	122	150
Nb	12	12	12

core rimmed by dioritic material of variable grain size. A hornblendite layer with pegmatoid biotite runs ENE–WSW in the northern part. The Pluton intrudes the Permian gabbroic rocks of the Mafic Complex (Ivrea–Verbano Zone). A pervasive network of more acidic veins and dykes marking the contact to the gabbro and the lack of metamorphic overprint should allow a clear distinction between the dioritic rocks of the Miagliano Pluton and the hydrothermally overprinted gabbros of the Ivrea–Verbano Zone (Carraro and Ferrara 1968).

Our analytical work focus on the central tonalitic portion of the intrusion (Table 1; the monzodiorite core of Carraro and Ferrara 1968). This part consists of quartz-dioritic to tonalitic rocks composed of white to greenish coloured plagioclase ($\sim$40–50 %), biotite ($\sim$15 %), amphibole ($\sim$15 %) and quartz ($\sim$15–20 %) with subordinate alkalifeldspar ($\sim$2 %), Fe–Ti oxides (ilmenite and magnetite 1–3 %), epidote + allanite ($\leq$1 %), fluorapatite ($\leq$1 %), and pyroxene ($\leq$1 %). In addition, zircon, pyrite, rutile, rare titanite and thorite occur as accessory constituents. The rock-forming minerals show in most localities a homogeneous grain size and magmatic texture, where only biotite and hornblende occasionally build slightly enlarged grains up to $\sim$4 mm without any solid state overprint. Chlorite and sericite occurs as alteration product after

biotite and amphibole. Hydrothermal alteration linked to very thin, cross-cutting quartz-filled veins is often attended by an increase in the content of Fe–Ti oxides and formation of coarse pyrite as well as a local production of calcite in the vicinity of the veins.

Biotite forms brownish to black lath-shaped or flat-tabular to sub-idiomorphic grains of $\leq$3–4 mm in size. The edges of the grains are regularly frayed and in part altered to chlorite ($\pm$sericite). Compositionally, two populations of biotite occur, characterized by different Mg, Fe^{2+} and Fe^{3+} exchange (Table 2). Biotite type 1 contains lower MgO ($\sim$11–12 wt%) in comparison to biotite type 2 (MgO $\sim$ 19–20 wt%). Both types of biotite contain $\sim$3.5 wt% TiO_2 similar to the low-Ti biotite in quartz diorite and gabbro norite related to the Valle del Cervo Pluton (Rosetti et al. 2007).

Amphibole (hornblende) forms $\leq$2 mm tabular to xenomorphic grains with green to pale brownish–yellow pleochroism. A number of hornblende grains contain a core with irregular domains of pyroxene (described below). Few larger grains of 4–5 mm in size exhibit a poikiloblastic texture with inclusions of Fe–Ti oxides, biotite, plagioclase, quartz, apatite and zircon. The amphiboles contain $\sim$6.64 Si pfu, $\sim$1 wt% TiO_2 and $\sim$0.6 wt% MnO (Table 2). Minor variations in composition are independent from the minerals in direct contact to the amphiboles. The Al^{tot} ranges from 1.3 to 1.9 pfu with octahedral site $Al^{VI} \sim 0.2$ pfu. The main compositional variations for the calcic amphiboles can be described by (1) the edenite exchange involving the substitution of Al for Si in the tetrahedral site coupled with Na and K substitution for vacancies in the A site and (2) $Fe^{2+} \Leftrightarrow Mg^{2+}$, (3) $Fe^{3+} \Leftrightarrow Al^{VI}$ and (4) Tschermak's (including Ti-Tschermak's) substitution on octahedral sites (Fig. 3). In addition, minor octahedral Mg $\Leftrightarrow$ Mn exchange occurs.

Pyroxene occurs as $\leq$300 μm large relict cores or irregular domains with distinct pyroxene cleavage and pale brownish colours in the hornblende grains. Boundaries to the hornblende are diffuse and irregular, and microprobe analyses show disturbed elemental distribution in the grains towards the boundary zones. Two distinct pyroxene compositions were identified: (1) Ca-rich clinopyroxene (augite, average composition: $En_{43}Fs_{23}Rho_1Wo_{24}Jad_1Esc_5$) with X_{Mg} ranging from 0.63 to 0.68, and (2) Ca-poor pyroxene (inverted pigeonite, average composition: $En_{49}Fs_{40}Rho_2Wo_3Jad_2Esc_3$) with X_{Mg} from 0.53 to 0.56 (Table 2). This suggests a two-pyroxene crystallisation sequence for the Miagliano tonalite. In addition, both pyroxenes contain little Al_2O_3 (1–4 wt%) and Na_2O ($\sim$0.2 wt%). Biotite and amphibole have rather similar X_{Mg} of 0.43–0.53, whereas the clinopyroxenes are noticeably richer in magnesium (augite: $X_{Mg} \sim$ 0.63–0.68 and pigeonite: $X_{Mg} \sim$ 0.53–0.56). This indicates that pyroxenes

Table 2 Average composition of the rock forming minerals

Mineral phase	Biotite[a]		Amphibole[b]		Pyroxene[c]	
Phase type	Low Mg (1)	High Mg (2)	Ca–Mg hornblende		Augite	Pigeonite
Number of analyses	152	55	52		13	26
Oxides (wt%)	Average	Average	Average	SD[d]	Average	Average
SiO_2	36.46	36.54	44.49	0.69	53.97	53.55
TiO_2	3.49	3.51	1.21	0.34	0.12	0.16
Al_2O_3	14.78	15.02	9.56	9.56	1.73	1.73
Fe_2O_3	4.84	4.45	6.07	1.04		
FeO	17.41	16.00	12.74	1.04	14.72	24.52
MnO	0.36	0.14	0.46	0.13	0.69	1.07
MgO	9.97	11.68	9.94	0.66	15.11	16.55
CaO	0.12	0.15	11.51	0.46	12.55	1.60
Na_2O	bdl	bdl	0.83	0.24	0.22	0.16
K_2O	9.94	9.34	0.90	0.18	0.09	0.04
H_2O	4.02	3.71	2.00			
Total	101.72	101.19	99.63		99.21	99.38
Cations (apfu)						
Si	2.619	2.605	6.640		2.046	2.062
Ti	0.188	0.188	0.136		0.003	0.005
Al^{tot}	1.251	1.262	1.682		0.078	0.078
Al^{IV}	1.251	1.262	1.360		0.005	0.001
Al^{VI}			0.322		0.073	0.077
Fe^{3+}	0.261	0.238	0.681			
Fe^{2+}	1.046	0.954	1.590		0.467	0.790
Mn	0.022	0.009	0.058		0.022	0.035
Mg	1.068	1.242	2.210		0.854	0.950
Ca	0.009	0.012	1.840		0.510	0.066
Na	0.012	0.024	0.239		0.016	0.012
K	0.911	0.849	0.172		0.004	0.002
H	0.825	0.666	2.000			
Total cations	7.391	7.387	15.247		4.000	4.000

The amphiboles are given with their standard deviation

[a] Biotite norm based on 11 oxygens and 2 (OH, F, Cl) using $Fe^{3+}/Fe_{tot} = 0.2$

[b] Amphibole norm based on 46 charges and $Fe^{3+}/Fe^{tot} = 0.3$. Normalization with 23 oxygens and Fe^{2+}/Fe^{3+} estimation assuming $\sum 13$ cations

[c] Pyroxenes normalized to 4 cations and 12 charges

[d] One standard deviation in wt%

have crystallised from a more mafic melt, and then, partially reacted to form amphibole during magma differentiation, as is often shown in tonalites.

Epidote contains high MgO content (~ 2.4 wt%; Fig. 4) and an average Fe_2O_3 content of ~ 8 wt% (Table 3). Compositions are comparable with other magmatic epidotes, except for MgO. In this context, the position of the Mg^{2+} cations in the epidote structure is not clear. The low sum of the measured oxides indicates traces of trivalent cations (i.e. REE^{3+}). However, Mg shows a weak correlation with Ca but no other elements, and in any case the A-site is filled with Ca (Fig. 4c).

Allanite forms xenomorphic grains of ≤ 300 μm in size. It occurs with two different textures: (1) small irregular grains and (2) larger concentrically zoned grains (Fig. 4). The latter are clearly resorbed, indicating instability and disequilibrium with the bulk tonalite chemistry. Thus, similar to the pyroxenes, these allanites may be xenocrysts formed in a precursor magma. Th content ranges from 0.03 to 1.69 wt% ThO_2 (average ~ 0.48 wt%). The total REE content of the allanite is in the range of 12.5–17.6 wt% REE oxides (Table 3). The allanite have a small dissakisite component as reported from other calc-alkaline intrusions (e.g., Gregory et al. 2009).
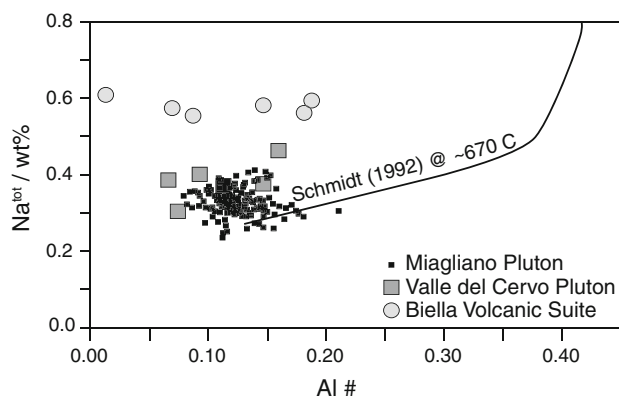
Fig. 3 Distribution of Al# [$=Al^4/(Al^6 + Al^4)$] versus $Na^{(tot)}$ in amphiboles from the tonalite of the Miagliano Pluton. Analyses from Valle del Cervo Pluton after Bigioggero et al. (1994), Biella volcanic suite after Callegari et al. (2004) are additionally shown

3.2 Pressure and temperature conditions for the emplacement of the Miagliano Pluton

The tonalite of the Miagliano Pluton includes the critical mineral assemblage necessary to employ the Al-in-hornblende barometer, i.e., quartz + plagioclase + K-feldspar + biotite + hornblende + magnetite (Fe–Ti oxides) + sphene (Hammarstrom and Zen 1986; Schmidt 1992). Thus, calculation of the crystallization pressure of the intrusion is based on this geobarometer. Calculations carried out on the average hornblende composition and hornblende rim compositions using the experimental calibration of Schmidt (1992) give pressures of 0.46 ± 0.06 GPa. The Anderson and Smith (1995) revised version of the Schmidt (1992) calibration give similar pressures ~0.46 GPa. This barometer considers the effect of temperature, for which we used the T calculated from Holland and Blundy (1994). Resulting temperatures have an uncertainty of ± 40 °C and yield values around 780 °C at the calculated pressure. The crystallisation temperature for the major mineralogy of the intrusion demonstrates little variation (~20 °C). The intrusion depth around 12 km for the Miagliano Pluton is thus clearly deeper than the 5–7 km depth inferred for the Valle del Cervo Pluton (Zanoni et al. 2008, 2010).

3.3 Field relation of the Valle del Cervo Pluton

The Valle del Cervo Pluton is a composite intrusion composed of concentrically ordered units that from rim to core include the Monzonitic complex, the Syenitic complex, the Pink Porphyric Monzogranite and the White Granite (Bigioggero et al. 1994). Major element bulk rock geochemistry and radiogenic isotopes indicate a mantle source for the primary melts followed by fractionation (Bigioggero et al. 1994; von Blankenburg et al. 1998). The
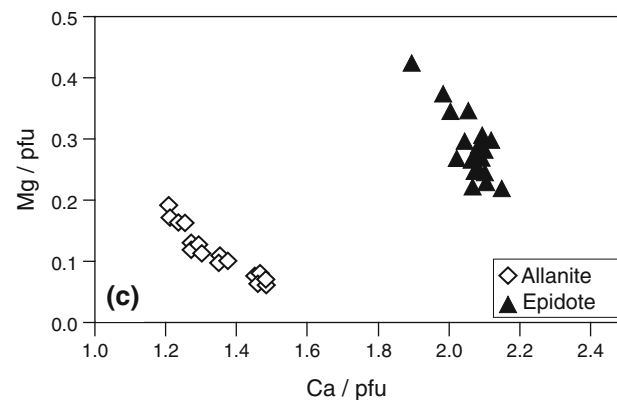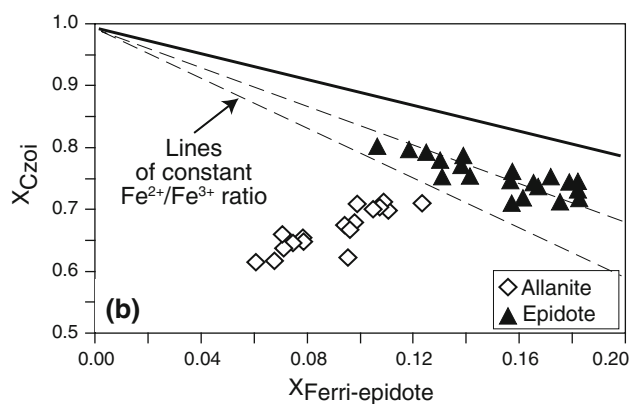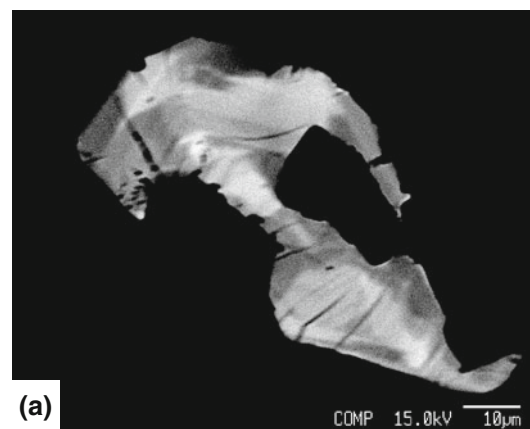
Fig. 4 Allanite composition and texture. **a** Resorbed and zoned allanite from the Miagliano tonalite (BSE image). **b** Data of allanite in $X_{Ferri-epidote}$ versus X_{Clzoi} diagram [$X_{Clzoi} = Al/(Al + Mg + Fe^{2+}+Fe^{3+})$; $X_{Ferri-epidote} = Fe^{3+}/(Al + Mg + Fe^{2+}+Fe^{3+})$]. **c** Ca versus Mg content in allanite and epidote. Note the high Mg content in the epidote

alkaline evolution for the different rock types as indicated by their major elements is outlined by the different Zr concentrations and zircon morphology (Caironi et al. 2000). Most of the zircon crystals have a magmatic morphology (Caironi et al. 2000), and the Zr concentration decreases from the monzonite to the granite (Fig. 2a), indicating achievement of early Zr saturation during the

Table 3 Representative analysis of epidote and allanite from the Miagliano Pluton

Mineral	Ep[a]	Ep[a]	Ep[a]	Aln[b]	Aln[b]	Aln[b]	Aln[b]
Oxide (wt%)							
SiO_2	37.07	36.72	37.16	33.19	33.94	34.73	34.63
TiO_2	0.70	0.15	0.14	0.52	0.39	0.25	0.21
ThO_2				1.36	0.87	0.09	0.09
Al_2O_3	22.76	23.95	23.53	17.46	18.45	21.06	21.08
Fe_2O_3	8.91	8.24	7.75	2.69	3.20	5.16	4.90
La_2O_3				6.20	5.48	3.36	3.51
Ce_2O_3				8.35	8.67	6.30	6.20
Pr_2O_3				0.69	0.76	0.66	0.70
Nd_2O_3				1.93	2.25	2.07	2.09
Sm_2O_3				0.08	0.19	0.33	0.23
Gd_2O_3				0.08	0.20	0.11	0.10
FeO				10.07	9.43	6.86	7.01
CaO	23.54	22.15	24.38	12.21	12.77	15.64	15.56
MgO	2.24	3.55	2.41	1.38	1.20	0.56	0.57
Sum	95.22	94.75	95.36	96.20	97.79	97.19	96.88
Cation (apfu)							
Si	2.975	2.929	2.957	3.066	3.067	3.022	3.022
Al	0.025	0.071	0.043				
$\sum$T-site	3.000	3.000	3.000	3.066	3.067	3.022	3.022
Al	2.128	2.181	2.164	1.901	1.965	2.160	2.168
Mg	0.268	0.422	0.286	0.190	0.161	0.073	0.074
Ti	0.042	0.009	0.008	0.036	0.027	0.016	0.014
Fe^{3+}	0.538	0.494	0.464	0.187	0.217	0.338	0.322
Fe^{2+}				0.778	0.713	0.499	0.511
$\sum$M1–3-site	2.976	3.107	2.921	3.091	3.083	3.086	3.089
Ca	2.024	1.893	2.079	1.208	1.236	1.458	1.455
Mn^{2+}				0.012	0.011	0.014	0.015
La				0.211	0.183	0.108	0.113
Ce				0.282	0.287	0.201	0.198
Pr				0.023	0.025	0.021	0.022
Nd				0.064	0.073	0.064	0.065
Sm				0.003	0.006	0.010	0.007
Gd				0.002	0.006	0.003	0.003
Th				0.029	0.018	0.002	0.002
U^{4+}				0.003	0.002	0.002	0.002
$\sum$A1–2-site	2.024	1.933	2.087	1.897	1.858	1.894	1.905

[a] Epidote norm based on 13 oxygens, 1 (OH, F, Cl) and $Fe^{3+}/Fe^{tot} = 1$

[b] Allanite norm based on 8 cations and 25 charges

magmatic evolution (Fig. 2b). As indicated by the contact metamorphic data (Zanoni et al. 2008, 2010), the Valle del Cervo Pluton intruded the HP rocks of the Mombarone nappe (in the Sesia–Lanzo Zone) at a depth of 5–7 km, corresponding to an emplacement pressure of 0.15–0.2 GPa.

3.4 Geochronology

The zircons from the Miagliano Pluton show typical magmatic habitus and zonation. Zonation was mapped by BSE and CL imaging on the SEM. The selected zoned crystals represent the majority of the grains. The magmatic zonation is in agreement with the scenario of crystallisation during fractionation and cooling of the calc-alkaline system (see below). The four single zircon grains measured by TIMS define an age scatter between 33.00 and 33.23 Ma; the youngest and concordant $^{206}Pb/^{238}U$ age of 33.00 ± 0.04 Ma is taken as approximation for the intrusion of the Pluton (Fig. 5; Table 4). The analyzed zircons are comparable in composition and age to the concordant zircons from the Biella Volcanic Suite (Fig. 5; Kapferer et al.
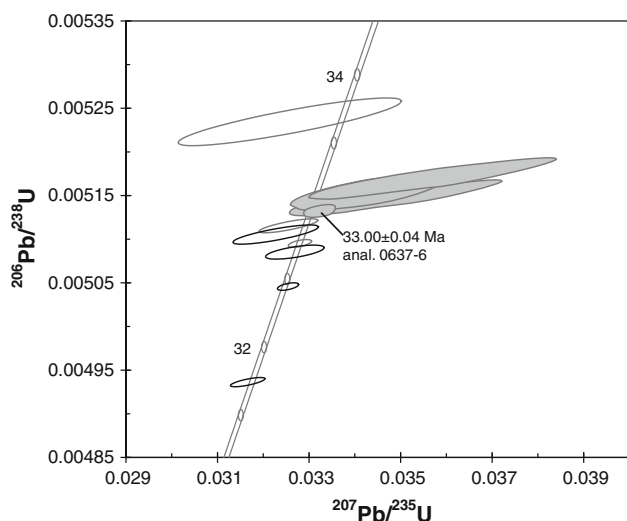
Fig. 5 Concordia diagram showing the results of zircon U–Pb dating of the calc-alkaline rocks. *Open ellipses* denote zircons form the BVS (Kapferer et al. 2012b), *filled ellipses* denote zircon from the Miagliano tonalite (this study). The used most concordant grain (*anal. 0637-6*) is indicated. Apparent upper intercept of 4,129 ± 670 Ma is meaningless

2012b). This Early Rupelian age is 10 my older than fission-track ages for zircon (23.5 ± 1.7 Ma) and apatite (19.0 ± 2.5 Ma; Berger et al. 2012).

For the Valle del Cervo Pluton ages already exist (Bigioggero et al. 1994; Romer et al. 1996). Samples were thus collected from the central granitic part of the Pluton (White Granite: Bigioggero et al. 1994). The small size of the Pluton, with an exposed diameter of ∼6 km total, and a country rock temperature in the range of 100–200 °C at the time of intrusion, do not allow large differences in crystallisation age from margin to centre. The six zircon crystals analyzed by TIMS are discordant, probably due to inherited cores. The lower intercept of 30.39 ± 0.50 Ma (Fig. 6; MSWD = 1.2) is interpreted as the crystallisation age of the intrusion.

3.5 Field relations, geochemical affinity and relative timing for emplacement of the dykes

In the Biella region, between the Upper Val Sessera and Valle dell'Elvo, several dykes of remarkable compositional diversity intrude the different tectonic units (Dal Piaz et al. 1979; Bigioggero et al. 1981, 1994; Beccaluva et al. 1983; Venturelli et al. 1984; Peccerillo and Martinotti 2006; Owen 2008; Conticelli et al. 2009). The MgO versus Zr diagram shows compositional trends for the collected samples of calc-alkaline, shoshonitic and ultrapotassic affinity as known from literature (Fig. 2; Dal Piaz et al. 1979; Bigioggero et al. 1981, 1994; Beccaluva et al. 1983; Venturelli et al. 1984; Peccerillo and Martinotti 2006;

Owen 2008; Conticelli et al. 2009), demonstrating the different evolution of each magmatic unit. The calc-alkaline suite shows increasing Zr content with magma differentiation (e.g., with decreasing MgO), whereas the shoshonitic suite is characterized by decreasing Zr with increasing degree of differentiation. The ultrapotassic dykes show a distinct variation in the Zr/MgO ratio. Combining the geochemical affinity with the field relationships of the dykes and the known temporal evolution of the Biella Volcanic Suite, Valle del Cervo Pluton and Miagliano Pluton, it is possible to establish a relative chronology for the emplacement of the various dykes.
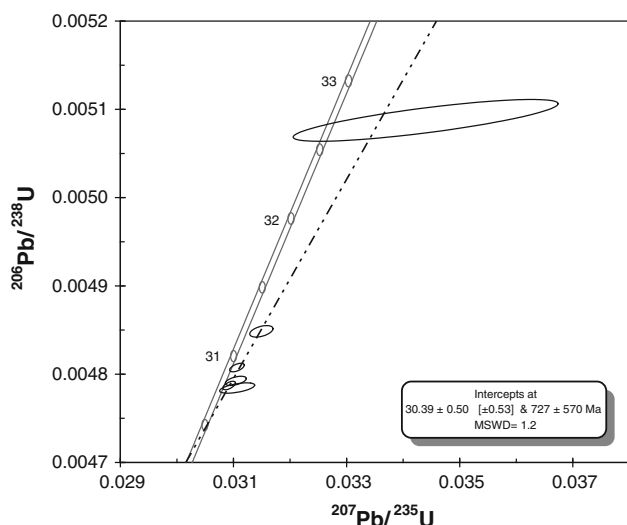
Two shoshonitic dykes cross-cutting the gneisses of the Sesia–Lanzo Zone and three calc-alkaline dykes in the upper Val Sessera were investigated in more detail (Figs. 2, 7). Near Bocchetta di Sessera, one of the shoshonitic dykes (Fig. 7a) discordantly intersects the main foliation of the gneisses (see also Plate 1 in Zanoni et al. 2008). The dyke is of andesitic composition and is strongly altered with typical surface type alteration dominated by Fe-oxides and hydroxides. One can follow the dyke until a few meters before the contact between the andesite of the Biella Volcanic Suite and the gneiss with a well-preserved paleosurface (Kapferer et al. 2012a). This is analogous to the detailed geological map of Zanoni et al. (2008), in which the dyke terminated at the contact with the extrusive andesite. Unfortunately, the field observations thus exclude a clear observation if the dyke is truncated by the paleosurface. However, the lack of strong alteration in a shoshonitic dyke of identical composition (Fig. 2a), intruding the gneiss several hundreds meter away from the paleosurface (Zanoni et al. 2008) argues for exposure of the aforementioned dyke prior to the emplacement of the andesite of the Biella Volcanic Suite. Furthermore, neither in this study nor reported in the literature have shoshonitic dykes cross-cut the rocks of the Biella Volcanic Suite. Consequently, at least part of the shoshonitic activity must predate the Rupelian emplacement of the calc-alkaline andesite (32.44–32.89 Ma, Kapferer et al. 2012b).

Bernardelli et al. (2000) describe a dyke cross-cutting the gneisses of the Sesia–Lanzo Zone south of the contact to the monzonite of the Valle del Cervo Pluton. The dyke shows strong hydrothermal alteration induced through a thickset network of quartz–carbonate veinlets. The hydrothermal activity is associated with the emplacement of the Valle del Cervo Pluton (Bernardelli et al. 2000), and thus the dyke is interpreted to be older than 30.4 Ma. Bellini et al. (1993) described an ultrapotassic sill (lamproite) intruding epiclastic rocks of the Biella Volcanic Suite. This indicates that strongly undersaturated magmas are emplaced after the main extrusive phase of the Biella Volcanic Suite. Two dykes intrude Ivrea-derived mylonites on the Southern Alpine side of the Canavese Line sensu

Table 4 Isotope measurements of single zircons

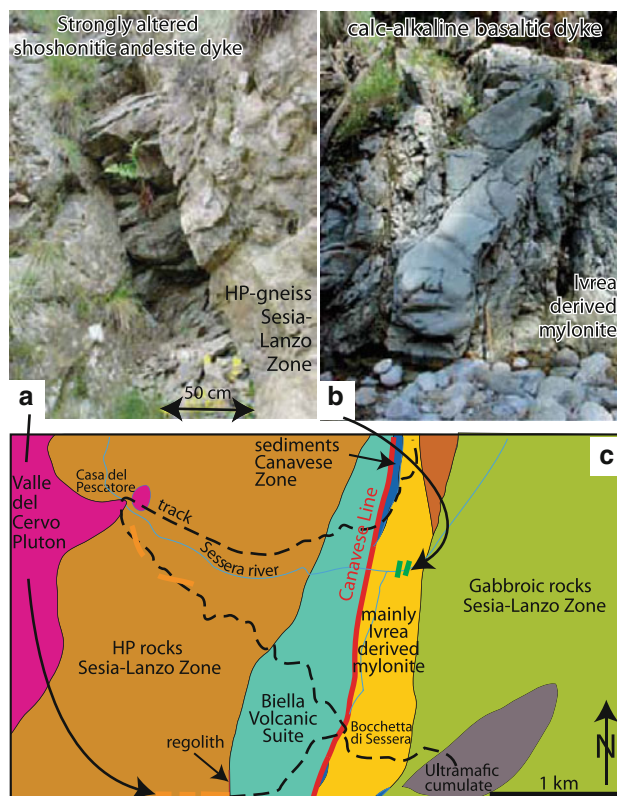| Number[a]	Concentrations					Atomic ratios								Apparent ages		
	Weight (mg)	U	Pb tot. (ppm)	Pb nonrad. (pg)	Th/U[b]	206/204[c]	207/206[d,e]	Error 2σ (%)	207/235[d,e]	Error 2σ (%)	206/238[d]	Error 2σ (%)	Corr.	206/238[e]	207/235	207/206[e]
Bi0632 (Valle del Cervo Pluton)																
0632-1	0.0014	280	2.35	1.21	0.49	121	0.04904	5.263525	0.03440	5.562495	0.00509	0.38	0.80	32.71	34.34	149.62
0632-2	0.0031	2,149	10.59	1.07	0.34	1,877	0.04686	0.300978	0.03106	0.339293	0.00481	0.08	0.56	30.92	31.06	42.02
0632-3	0.0029	1,867	9.13	1.40	0.20	1,187	0.04711	0.491792	0.03149	0.532045	0.00485	0.11	0.46	31.18	31.48	54.70
0632-4	0.0022	2,443	11.83	1.29	0.22	1,259	0.04698	0.448604	0.03104	0.48726	0.00479	0.09	0.51	30.82	31.04	48.01
0632-5	0.0024	1,029	5.09	1.05	0.18	723	0.04709	0.763705	0.03106	0.814178	0.00478	0.10	0.55	30.77	31.06	53.85
0632-6	0.0030	3,724	17.62	1.53	0.23	2,197	0.04685	0.254175	0.03092	0.294442	0.00479	0.08	0.60	30.79	30.92	41.49
Bi0637 (Miagliano Pluton)																
0637-2	0.0047	125	1.22	2.5	0.59	95	0.05012	5.86	0.03572	6.20	0.00517	0.38	0.91	33.23	35.63	200.56
0637-3	0.0020	469	4.29	3.4	0.62	108	0.04921	5.15	0.03492	5.44	0.00515	0.32	0.91	33.09	34.85	157.68
0637-5	0.0025	167	1.30	1.0	0.57	159	0.04829	3.85	0.03431	4.06	0.00515	0.32	0.70	33.13	34.25	113.31
0637-6	0.0040	564	3.33	1.0	0.59	712	0.04699	0.81	0.03324	0.86	0.00513	0.12	0.46	33.00	33.21	48.50

[a] All zircons annealed-leached, all single grains

[b] Calculated on the basis of radiogenic Pb^{208}/Pb^{206} ratios, assuming concordancy

[c] Corrected for fractionation and spike

[d] Corrected for fractionation, spike, blank and common lead (Stacey and Kramers 1975)

[e] Corrected for initial Th Disequilibrium, using an estimated Th/U ratio of 4 for the melt

Fig. 6 Concordia diagram with the results of zircon U–Pb dating of the Valle del Cervo Pluton

Fig. 7 Field relations of dyke emplacement: **a** shoshonitic andesitic dyke crosscutting the high pressure gneiss of the Sesia–Lanzo Zone, showing strong surface alteration and being probably truncated by the formation of the Early Rupelian (see also Zanoni et al. 2008, their Fig. 2a and Plate 1); **b** calc-alkaline basaltic dyke intruding the Ivrea derived mylonite; the dyke only suffered late brittle deformation; **c** map of the area of the upper Val Sessera showing the location of the dykes (**a**) and (**b**)

strictu (mylonite belt 1 of Schmid et al. 1989) in the upper Val Sessera at Piana del Ponte (Fig. 7). These dykes are basaltic to trachy-basaltic in composition with a calc-alkaline affinity (Fig. 2). They show an intersertal (doleritic) microstructure and pervasive hydrothermal alteration (with quartz, calcite, chlorite and epidote). The two dykes have the same composition as the dioritic proportion in the Miagliano Pluton (Fig. 2a). They intrude sub-parallel to the mylonitic foliation of strongly deformed and partly hydrothermally altered rocks originating from the Ivrea–Verbano Zone. One of the dykes is essentially undeformed (Fig. 7), whereas the other one (outcropping 150 m west of the first dyke) is partially dismembered and slightly foliated, and has developed a new foliation. Schmid et al. (1989) analyzed the magnetic orientation of the undeformed dyke and suggested a rotation of ca. 60° along NNE–SSW oriented sub-horizontal axes. Bigioggero et al. (1981) described similar doleritic dykes cross-cutting Late Hercynian granitoids of the Serie dei Laghi south of the Cremosina Line (see Fig. 1). Based on preliminary paleomagnetic data, they suggested a rotation of ca. 20°–30° for the dykes.

If the calc-alkaline geochemistry of the dyke-like intrusions in the Ivrea–Verbano Zone and the Canavese Line mylonite is a robust genetic link to the Miagliano Pluton, then an Early Rupelian age for these rocks can be inferred. Furthermore, if this age is correct, then the mylonitic belt is reactivated during the post-Rupelian period. This deformation is associated with a strong hydrothermal overprint at lower greenschist facies conditions. It is important to note, that volcanic rocks of calc-alkaline and shoshonitic affinity coexist in the epiclastic

conglomerates of the Biella Volcanic Suite together with clasts from the Sesia–Lanzo Zone (Callegari et al. 2004; Kapferer et al. 2012b). This clearly indicates contemporaneous presence of all three units at the erosion surface in Early Rupelian times. The age relationships of shoshonitic dykes discussed above indicate a first shoshonitic activity predating the calc-alkaline one, and then, 2 Ma later, a second shoshonitic magma impulse ascended to the upper crust, emplacing the intrusion of the Valle del Cervo Pluton.

In summary: a first suite of shoshonitic dykes intrudes the Sesia–Lanzo Zone before the formation of the regolith in Early Rupelian times. The basaltic calc-alkaline dykes in the Ivrea–Verbano Zone seem to be closely related to the intrusion of the Miagliano Pluton and with the calc-alkaline andesitic volcanic rocks of the Biella Volcanic Suite and therefore of Mid Rupelian age (32.5–32.9 Ma). The lamproitic dyke described by Bellini et al. (1993) is the youngest one, because it intrudes the epiclastic rocks of the Biella Volcanic Suite.

4 Discussion

4.1 Comparison of the age data with published ages

The zircon age of the Miagliano Pluton (33.00 ± 0.04 Ma) represents the emplacement age of the pluton. Published Rb/Sr and K/Ar ages obtained on biotite (29–33 Ma with a median of 31 Ma; Carraro and Ferrara 1968) overlap within error our zircon U/Pb age. Therefore, these geochronometers were not reset during cooling of the Pluton. The Valle del Cervo Pluton age of 30.39 ± 0.50 Ma overlaps with published Rb/Sr biotite isochron ages (29.0 ± 0.5–31.0 ± 0.5 Ma; Bigioggero et al. 1994) and with the zircon U/Pb age of 31.0 ± 0.20 Ma obtained by Romer et al. (1996). As mentioned above, the Valle del Cervo Pluton cooled in time ranges of ka, which is in the analytical error of the isotope data. The order of time range of solidification is independent of the position of the sample inside the Pluton (rim or core). In contrast to overlapping K/Ar biotite ages with emplacement ages of both Plutons, the zircon and apatite fission-track ages are significantly younger (Kapferer 2010; Berger et al. 2012).

4.2 Magmatic evolution and high precision ages

The mineralogical and geochemical characteristics of the Miagliano tonalite fit into the calc-alkaline differentiation pathway of the Western Alps (i.e. Biella Volcanic Suite, Traversella Pluton, calc-alkaline dykes; Fig. 2). The magmatic evolution can be described in terms of fractionation from a mantle melt and assimilation of a crustal component (e.g., von Blankenburg et al. 1998). In this context, the Miagliano Pluton represents a small (i.e., a few km^3) tonalitic/dioritic batch of a larger coeval magmatic activity, emplaced at intermediate crustal depth (ca. 12 km). The differentiation of the magma is indicated in the tonalite by the occurrence of relicts such as the pyroxene inclusions in the amphibole, which have crystallized in a more primitive melt, and the resorbed allanites representing relics not stable in the matrix of the crystallizing tonalitic melt (Fig. 4). Such evidences of disequilibrium are crucial to understand the behaviour of REE and Th/U ratios during the differentiation of magmatic systems, including the chronometers. The most useful scenario for the interpretation of single grain zircon ages is the situation of zircon saturation during magma evolution (e.g., Schaltegger et al. 2009). This can be expected in calc-alkaline systems, where primary mafic melts are undersaturated in Zr, and saturation (and thus zircon fractionation) will only be achieved through fractionation and cooling. For the calc-alkaline rocks, the Th/U ratio of the zircons decreases with age (Fig. 8a), which is a common phenomena in such magmatic systems (e.g., Schaltegger et al. 2009). The

difference in Th/U ratio can be assigned to fractionation of a phase with a high Th content such as allanite (e.g., Oberli et al. 2004) or titanite (Schaltegger et al. 2009). The potential processes of fractionation may be deciphered by the chemical, isotopic and age constrains from the volcanic and Plutonic equivalents (see also Gagnevin et al. 2010). The variation of the Th/U ratio in the investigated zircons of the Miagliano Pluton is small (Fig. 8a). In contrast, the single grain zircon ages of the volcanic Biella Suite are concordant and cover a certain spread in Th/U ratios (Fig. 8a; Kapferer et al. 2012b). The change in Th/U ratio of the zircon grains with time (Fig. 8a) is interpreted as related to the fractionation of a Th-rich phase like allanite in the evolving magma reservoir. The allanite xenocrysts in the Miagliano tonalite show signs of such a process, as most allanite grains in the plutonic rock are resorbed (Fig. 5). This demonstrates disequilibrium conditions for allanite with respect to the melt evolving towards the present tonalitic composition. In addition, they have a significant dissaksite component, indicating crystallisation in a more Mg-rich, primitive system. Similarly, early fractionation of a Th-rich phase would explain the temporal decrease of the Th/U ratio and MgO content in the bulk rock composition of the calc-alkaline as well as of the alkaline suites (Fig. 8b). The occurrence of allanite during partial melting and fractionation in calc-alkaline systems has been shown for natural and experimental systems (e.g., Hermann 2002; Gregory et al. 2009). However, the general trend of increasing LREE during fractionation of calc-alkaline suite is contradictory to pure fractionation of allanite. The change in Th/U ratio may be related to a late stage, whereas the earlier evolution from a basaltic to a granodioritic composition mainly include fractionation of clinopyroxene and assimilation of a crustal component.

The new dating results combined with the field-based relative chronology of dyke emplacement establish the evolution of geochemical distinct magmatic systems within a restricted temporal and spatial frame. The Miagliano Pluton intrudes the rocks of the Ivrea–Verbano Zone at 12–15 km depth around 33 Ma. At nearly the same time (32.5 Ma; Kapferer et al. 2012b) calc-alkaline and shoshonitic volcanic rocks were deposited on the surface of the Sesia–Lanzo Zone. Some of the shoshonitic dykes probably predate the extrusion of the Biella Volcanic Suite, and were subsequently followed (at 30.5 Ma) by the intrusion of the shoshonitic Valle del Cervo Pluton.

4.3 Geodynamic evolution

The magmatic rocks studied herein do not just exhibit a distinct magmatic evolution, but have significantly different emplacement depths: (1) Biella Volcanic Suite surface extrusion; (2) Valle del Cervo Pluton 5–7 km depth; and

Fig. 8 **a** Th/U ratio versus the U/Pb age of the single grain zircon ages (Table 4). **b** Th/U ratio versus MgO of the whole rocks (data source: Venturelli et al. 1984; Van Marcke de Lumen and Vander Auwera 1990; Owen 2008; Conticelli et al. 2009). In addition the Th/U ratios of Cesana et al. (1976) are indicated as *boxes* as no exact MgO values are available. **c** Whole rock La versus MgO for the calc-alkaline rocks (data source as in **a**). **d** Whole rock $^{87}Sr/^{86}Sr$ isotope ratios versus MgO of dykes of the Sesia–Lanzo Zone. Data source: Bergell-Adamello trend: Kagami et al. (1991); von Blanckenburg et al. (1992, 1998); Venturelli et al. (1984); Owen (2008); Conticelli et al. (2009)

(3) Miagliano Pluton 12–15 km depth. The differences in emplacement depth were reorganized during post Rupelian times by rigid block rotation (Schmid et al. 1989; Berger et al. 2012). The block rotation includes burial of the Biella Volcanic Suite and exhumation of the Miagliano Pluton. The burial of the Biella Volcanic Suite surface rocks to depths of 5–7 km is indicated by the rejuvenation of the fission tracks and by the low-grade metamorphic overprint of the rocks (Zingg et al. 1976; Kapferer et al. 2012b). The burial occurred during 2 Ma, constrained by the age of the volcanic rocks (32.5 Ma) and the intrusion age of the Valle del Cervo Pluton (30.5 Ma). Thus, as indicated by the exposed geometry of the two units, the burial of the volcanic rocks must predate the intrusion of the Valle del Cervo Pluton (Fig. 1). The present day shortest distance between the Pluton and volcanic rocks is 0.7 km (Valle del Cervo), which is much less than the estimated intrusion depth of 5–7 km for the Valle del Cervo Pluton (Zanoni et al. 2008, 2010). This can only be explained by a re-burial of the Sesia Zone to depth of ∼5 km prior to the intrusion of the Pluton. On the eastern side of the Canavese Line, the Miagliano Pluton (which is 2.4 Ma older than the Valle del Cervo Pluton and coeval to the Biella Volcanic Suite) underwent single exhumation from a deeper level and over a longer time span, as indicated by the zircon and apatite fission-track ages (Berger et al. 2012).

Hence, to combine the alkaline magmatic evolution and calc-alkaline evolution, quick changes in the upper crust geometry is required. The evolution of the Tertiary calc-alkaline suites of the Alps is consistently governed by AFM processes, where primitive melts from a depleted mantle source assimilate significant proportions of lower and upper crustal components (more then 30 % crustal melts; detailed modelling in von Blanckenburg et al. 1992, 1998; and Thompson et al. 2002 for the Adamello-Pluton). In contrast, the alkaline magmatism is relatively primitive in terms of major element composition (i.e. Mg#, Fig. 8d), but require a complex melt source (e.g., Sr, Nd; Fig. 8; Owen 2008; Conticelli et al. 2009; Tommasini et al. 2011). Tommasini et al. (2011) present a model to explain the chemistry of such Tethyan lamproites. They focused on a so-called "SALATHO" reservoir in the melting area
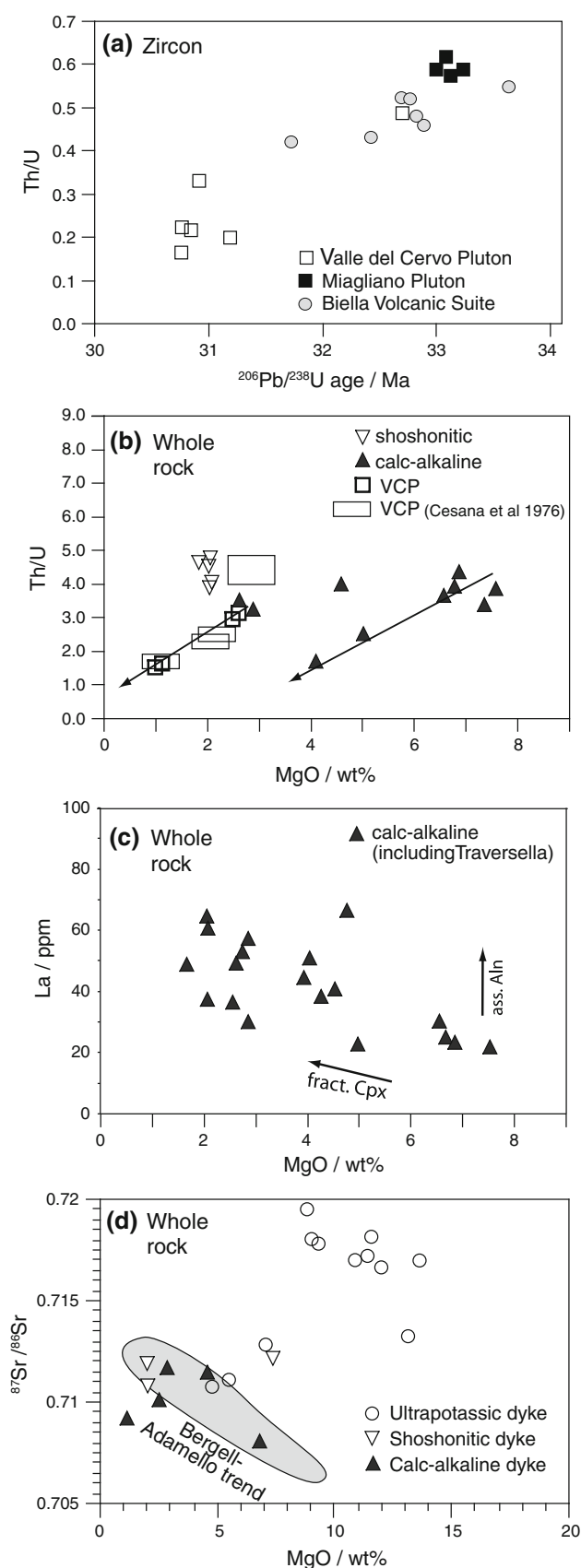
characterized by high Sm/La and Th/La ratios of the mantle (Tommasini et al. 2011). The origin of such a reservoir in the mantle is explained by a first stage of HP/LT metamorphism including lawsonite and zoisite/epidote veins transported into the mantle. To explain the K-component in the mantle, a second step was proposed, producing K-rich melts that migrated through the mantle wedge and metasomatised it (Tommasini et al. 2011). REE patterns, Th/La and Sm/La ratios differ for the lamproites and calc-alkaline members of the Western Alps (Fig. 9).
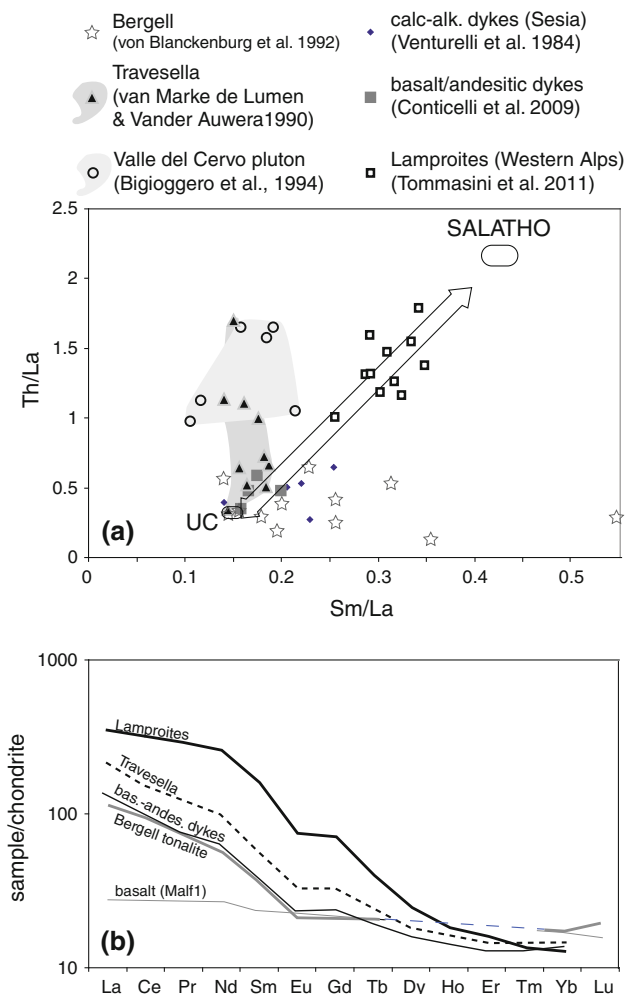
Fig. 9 a Th/La ratio versus the Sm/La ratio redrawn from Tommasini et al. (2011). SALATHO = assumed reservoir with certain Th/La and Sm/La ratios; *UC* upper crust. In addition data from the Bergell pluton (calc alkaline evolution, von Blanckenburg et al. 1992); basaltic-andesitic dykes (Venturelli et al. 1984; Conticelli et al. 2009); Val Cervo Pluton (Bigioggero et al. 1994) are shown (**b**). REE pattern of the different groups of alkaline and calc-alkaline evolution in the Alps. *Bold line* average of ultrapotaasic dykes of Conticelli et al. 2009; *black thin line* average of basaltic/andesitic dykes (Conticelli et al. 2009); *black stippled line* Travesella diorite (Van Marcke de Lumen and Vander Auwera 1990); *grey thick line* Bergell tonalite (von Blanckenburg et al. 1992); *grey thin line* Bergell basalt (von Blanckenburg et al. 1992)

However, the REE-patterns for the calc-alkaline rocks of the whole Alps are comparable. In contrast, the Th/La trend is different for calc-alkaline rocks of the Western Alps to the central Alps (e.g., Bergell Pluton; Fig. 9). This requires different sources and/or a different melt evolution in the Western Alps compared to the central and eastern Alps. A refined view on the situation sketched by Tommasini et al. (2011) would include a plate tectonic boundary between the Western Alps and the central Alps in order to explain the difference in chemical evolution for these two areas. Such a plate tectonic strike slip boundary has been proposed by several authors (e.g., Ricou and Siddans 1986; Handy et al. 2010; Dumont et al. 2011). This boundary explains the different evolution between the western- and the central-Alps. In contrast to the central Alps, the western Alpine lithospheric section includes numerous tectonic slices accreted through the different subduction and exhumation events and superimposed along the same suture (Fig. 10; i.e., Sesia subduction is missing in the central Alps; Berger and Bousquet 2008). In addition, the Jurassic rifting exhumed Palaeozoic sub-continental mantle along shear zones, which later were reactivated during the Late Cretaceous (Babist et al. 2006 and references therein). Even omitting Palaeozoic metasomatic alterations, it is evident that during these two antithetic events a portion of the respective hanging wall was affected by infiltration of different fluids, originating from the lower plate. During Jurassic rifting, sub-continental mantle was exhumed to the surface (northern ocean–continent transition zone of the
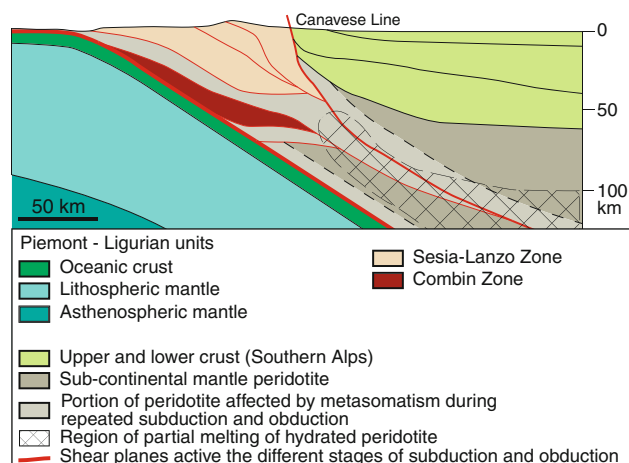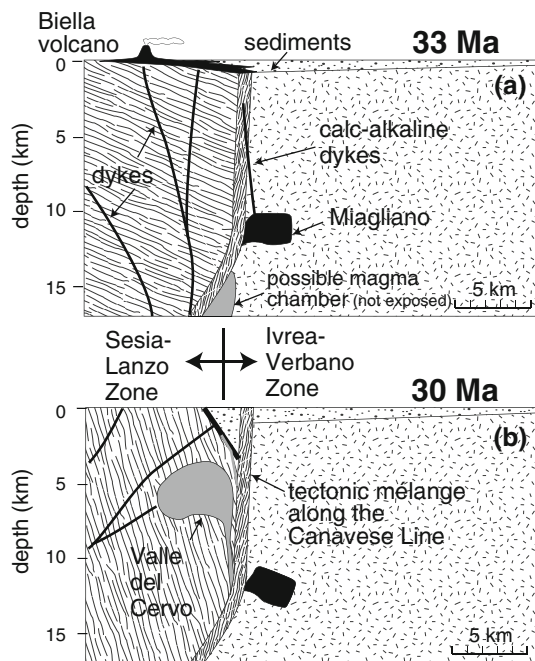

Fig. 10 Schematic profile (present day orientation roughly NW–SE) through the internal Western Alps in Rupelian times (inspired by Babist et al. 2006, their Fig. 10f) showing the position in the upper plate of the subduction zone of different portion of mantle peridotites having suffered distinct kinds of metasomatic alteration (see text for discussion). These represent potential sources for the generation of the primitive melts of the heterogeneous Oligocene magmatism in this area. The position of the melting zone have been located following current thermal model for the alpine subduction (e.g., Stöckhert and Gerya 2005)

Adriatic plate; Ferrando et al. 2004) and underwent hydration. This is different to the situation in the central- and eastern-Alps, but can be compared with the first stage proposed by Tommasini et al. (2011).

Decompression in the lower exhuming plate may have generated melts able to infiltrate the upper plate. During Late Cretaceous convergence the hydrated oceanic mantle subducted, followed by the continental units (i.e. Sesia–Lanzo). Dehydration and melting in these units produced an alteration front in the mantle rocks of the hanging plate. Late Cretaceous calc-alkaline magmatism related to this subduction is unknown in the Alps, except for some rare volcanic clasts in the Schlieren Flysch of Maastrichtian to Palaeocene age (Winkler 1983). In Eocene, the continental HP rocks were exhumed along the same suture zone to the surface, whereas at the same time, the oceanic Piemont–Liguria lithosphere was subducted. The exhumed Sesia–Lanzo Zone became the frontal part of the upper plate and the mantle wedge below the Sesia–Lanzo Zone was formed by a complex patchwork of differently altered peridotitic slices bounded by shear zones. The most prominent of these shear zone is the Canavese Line (Figs. 10, 11). At depths between 50 and 150 km, this tectonic evolution created the compositional prerequisites for the generation of the different primitive melts parental to the Oligocene

Fig. 11 Sketch of the time–space evolution around the Canavese Line (see also Schmid et al. 1989). **a** Around 33 Ma the calc-alkaline rocks of the BVS emplaced on the paleosurface of the Sesia–Lanzo Zone while the Miagliano Pluton intrudes the Ivrea–Verbano Zone. **b** Around 30 Ma the Valle del Cervo Pluton intrudes at upper crustal level during the rigid block rotation responsible for the burial of the Biella Volcanic Suite

magmatic rocks. Furthermore, Fig. 10 shows that applying a conventional thermal structure for subduction zones, a large volume of the metasomatically altered mantle fit into the melting field for hydrated peridotite (T > 1,200 °C; for isotherms see for example Stöckhert and Gerya 2005). The lithospheric scale mylonitic belt related to the different movements along the Canavese Line provides the structural path for the ascent of the melts (Rosenberg 2004).

The calc-alkaline activity is produced by the typical subduction-related magmatism, associated with partial melting of hydrated, depleted mantle occurring at 50–100 km depth. The primary basaltic melts produced underwent fractionation and assimilation of crustal material in different magma reservoirs during ascent. The inherited xenocrysts of pyroxene and allanite in the Miagliano Pluton are relics of such processes. This activity is, on the scale of the entire Alps, by far the volumetrically most prominent. At least for the Western Alps section it is thus not necessary to invoke slab break-off to generate the calc-alkaline melts (Fig. 10). The alkaline activity is more localized and volumetrically subordinate. In the internal Western Alps, with the Valle del Cervo Pluton and the numerous ultrapotassic dykes, the frequency of alkaline rocks is higher than in other areas of the Alps. The existence of a strongly metasomatized mantle slice in the upper plate of the subduction zone is a result of the tectonic history of the area, and these slices can be seen as potential source regions for the primitive alkaline melt. Thus, (1) difference in intensity and type of metasomatic alteration of the mantle rocks, (2) the spatial distribution of the altered mantle portions in the melting volume and, (3) varying degree of partial melting, are considered to be responsible for the compositional variation of the primary melts and for the described magmatic rocks (lamproite, minette, spessartite, kersantite; Owen 2008; Conticelli et al. 2009). Fractionation of magma batches during ascent lead to the different lithotypes of the Biella Volcanic Suite (Callegari et al. 2004) and Valle del Cervo Pluton (Bigioggero et al. 1994). The relative chronology of the alkaline rocks (Fig. 11) indicates: (1) they may predate the calc-alkaline volcanism; (2) they can be coeval with them and, (3) they are younger as seen for the Valle del Cervo Pluton. Thus, we suggest that the calc-alkaline magmatism in the Western Alps represents a more short-lived episode characterized by the production of fairly large volumes of melt, whereas the alkaline rocks are produced by cyclic, small volume and localized melting events.

5 Conclusions

Precise radiometric dating of the magmatic rocks outcropping in a restricted area around Biella, combined with their

depth of emplacement and the relative chronology issued from field observations, constrain the evolution of the orogenic magmatism in the internal Western Alps to a short period of time in the first half of the Rupelian. The calc-alkaline Miagliano Pluton intruded the Permian gabbroic rocks of the Ivrea–Verbano Zone during Early Rupelian (33.00 ± 0.04 Ma) at a depth of 12–15 km just southeast of the Canavese Line (Fig. 11). Mineral compositions demonstrate fractionation as governing mechanism for the evolution of this pluton. Basaltic dykes of very similar composition are assumed to be co-genetic and coeval with the Miagliano Pluton. Two of the dykes intruded the Ivrea derived mylonite occurring along the Canavese Line, and were subsequently slightly deformed. The calc-alkaline andesite of the Biella Volcanic Suite outcropping just northwest of the Canavese Line are insignificantly younger (32.44–32.89 Ma) than the Miagliano Pluton. However, epiclastic conglomerates from the Biella Volcanic Suite units do, besides calk-alkaline clasts, also contain shoshonitic volcanic rocks and HP gneisses. Hence, volcanic edifices of both magmatic series were exposed contemporaneously and at the same erosional level. One of the shoshonitic dykes seems to be truncated by the regolith on top of the Sesia gneisses and is superimposed by calc-alkaline andesite. Within less than 2 Ma, the paleosurface including the Biella Volcanic Suite is buried to a depth of 5–7 km, the intrusion depth of the Valle del Cervo Pluton. The crystallisation age (30.39 ± 0.50 Ma) of the Valle del Cervo Pluton marks the end of the upper-crustal rigid block rotation responsible for the burial of the Biella Volcanic Suite (Fig. 11). Therefore, in the internal Western Alps, the orogenic magmatism seems to be restricted to the first half of the Rupelian. This is supported by the age of the Traversella Pluton of 30 Ma (Krummenacher and Evernden 1960) and by a lamprophyre near Brusson yielding an age of 33 Ma (Pettke et al. 1999; L. Diamond, pers. com.). The only exception to this age range is a 44 Ma old andesitic dyke from Val Chiusella (Babist et al. 2006). This paroxysm of the magmatic activity is linked, at least for its upper crustal expression, to differential rigid blocks movement including rotation, and affecting the Sesia–Lanzo Zone as well as the Ivrea–Verbano Zone. Aquitanian zircon and apatite fission-track ages for the Miagliano Pluton and Burdigalian–Langhian ages for the Valle del Cervo Pluton and the Biella Volcanic Suite indicate that the differential uplift continued into the Early Miocene.

References

Anderson, J. L., & Smith, D. R. (1995). The effects of temperature and fO_2 on the Al-in-hornblende barometer. *American Mineralogist, 80*, 549–559.

Babist, J., Handy, M. R., Konrad-Schmolke, M., & Hammerschmidt, K. (2006). Precollisional, multistage exhumation of subducted continental crust: the Sesia Zone, western Alps. *Tectonics, 25*, TC6008.

Beccaluva, L., Bigioggero, B., Chiesa, S., Colombo, A., Fanti, G., Gatto, G. O., et al. (1983). Post collisional orogenic dyke magmatism in the Alps. *Memorie della Societa Geologica Italiana, 26*, 341–359.

Bellini, A., Callegari, E., Compagnoni, R., & Ruffini, R. (1993). Prima segnalazione di rocche ultrapotassiche a leucite nelle Alpi Occidentali. *Plinius, 10*, 41–43.

Berger, A., & Bousquet, R. (2008). Subduction-related metamorphism in the Alps: review of isotopic ages based on petrology and their geodynamic consequences. In S. Siegesmund, B. Fügenschuh & N. Froitzheim (Eds.), *Tectonic aspects of the Alpine-Dinaride-Carpathians System* (Vol. 298, pp. 117–114). London: Geological Society of London Special Publication.

Berger, A., Mercolli, I., Kapferer, N., & Fügenschuh, B. (2012). Single and double exhumation of fault blocks in the internal Sesia–Lanzo Zone and the Ivrea–Verbano Zone (Biella, Italy). *International Journal of Earth Science,.* doi:10.1007/s00531-012-0755-6.

Bernardelli, P., Castelli, D., & Rossetti, P. (2000). Tourmaline-rich ore-bearing hydrothermal system of lower Valle del Cervo (Western Alps, Italy): field relationships and petrology. *Schweizerische Mineralogische Petrographische Mitteilungen, 80*, 257–277.

Bigi, G., Castellarin, A., Coli, M., Dal Piaz, G. V., Sartori, R., Scandone, P., & Vai, G. B. (1990). Structural model of Italy, sheet 1. C.N.R., 1: 500,000. Progetto finalizzato geodinamica, SELCA Firenze.

Bigioggero, B., Colombo, A., Del Moro, A., Gregnanin, A., Macera, P., & Tunesi, A. (1994). The Oligocene Valle del Cervo Pluton: an example of shoshonitic magmatism in the western Italian Alps. *Memorie della Societa Geologica Italiana, 46*, 409–421.

Bigioggero, B., Colombo, A., Lanza, R., & Sacchi, R. (1981). Dati geochimici e paleomagnetici preliminari su filoni del sudalpino della zona del Biellese. *Rendiconti Societa Geologica Italiana, 46*, 271–274.

Bonin, B. (2004). Do coeval mafic and felsic magmas in post-collisional to within-plate regimes necessarily imply two contrasting, mantle and crustal, sources? A review. *Lithos, 78*, 1–24.

Bortolami, G., Carraro, F., & Sacchi, R. (1965). Le migmatiti della Zona Diorito-kinzigitica nel Biellese ed il loro inquadramento geotettonico. Nota preliminare. *Bollotino della Societa Geologica Italiana, 84*, 5–21.

Caironi, V., Colombi, A., Tunesi, A., & Gritti, C. (2000). Chemical variation of zircon compared with morphological evolution during magmatic crystallisation: an example from the Valle del Cervo Pluton. *European Journal of Mineralogy, 12*, 779–794.

Callegari, E., Cigoli, C., Medeot, O., & D'Antonio, M. (2004). Petrogenesis of calc-alkaline and shoshonitic post-collisional oliocene volcanics of the Cover-Serie of the Sesia zoine, western Italian Alps. *Geodynamica Acta, 17*, 1–29.

Carraro, F., & Ferrara, G. (1968). Alpine "tonalite" at Miagliano, Valle del Cervo (Zona dioritica–kinzigitica): a preliminary note. *Schweizerische Mineralogische und Petrographische Mtteillungen, 48*, 75–80.

Cesana, A., Demonte, L., & Venegoni, M. (1976). Origin of the Cervo pluton according to the U and Th content and distribution.

Rendiconti Societa Italiana Mineralogia Petrologica, 32, 637–646.

Conticelli, S., Guarnieri, L., Farinelli, A., Mattei, M., Avanzinelli, R., Bianchini, G., et al. (2009). Trace elements and Sr–Nd–Pb isotopes of K-rich, shoshonitic, and calc-alkaline magmatism of the western Mediterranean region: genesis of ultrapotassic to calc-alkaline magmatic associations in a post-collisional geodynamic setting. *Lithos, 107*, 68–92.

Dal Piaz, G. V., Venturelli, G., & Scolari, A. (1979). Calc-alkaline to ultrapotassic postcolliional volcanic activity in the internal northwestern Alps. *Memorie della Science Geologica, 32*, 1–16.

De Capitani, L., Fiorentini Potenza, M., Marchi, A., & Sella, M. (1979). Chemical and tectonic contributions to the age and petrology of the Canavese and Sesia–Lanzo "porphyrites". *Atti Società Italiana di Scienze Naturali, 120*, 151–179.

Dumont, T., Simon-Labric, T., Authemayou, C., & Heymes, T. (2011). Lateral termination of the north directed Alpine orogeny and onset of westward escape in the western Alpine arc: structural and sedimentary evidence from the external zone. *Tectonics, 30*, TC5006.

Ferrando, S., Bernoulli, D., & Compagnoni, R. (2004). The Canavese zone (internal western Alps): a distal margin of Adria. *Schweizerische Mineralogische Petrographische Mitteilungen, 84*, 237–256.

Gagnevin, D., Daly, S. J., & Kronz, A. (2010). Zircon texture and chemical composition as a guide to magmatic processes and mixing in a granitic environment and coeval volcanic system. *Contribution to Mineralogy and Petrology, 159*, 579–596.

Giese, J., Seward, D., Stuart, F. M., Wüthrich, E., Gnos, E., Kurz, D., et al. (2010). Electrodynamic disaggregation: does it affect apatite fission-track and (U–Th)/He analyses? *Geostandards and Geoanalytical Research, 34*, 39–48.

Gregory, C. J., McFarlane, C. R. M., Hermann, J., & Rubatto, D. (2009). Tracing the evolution of calc-alkaline magmas: In situ Sm–Nd isotope studies of accessory minerals in the Bergell Igneous Complex, Italy. *Chemical Geology, 260*, 73–86.

Hammarstrom, J. M., & Zen, E-an. (1986). Aluminium in Hornblende: an empirical igneous geobarometer. *American Mineralogist, 71*, 1297–1313.

Handy, M. R., Schmid, S. M., Bousquet, R., Kissling, E., & Bernoulli, D. (2010). Reconciling plate-tectonic reconstructions of Alpine Tethys with the geological–geophysical record of spreading and subduction in the Alps. *Earth-Science Reviews, 102*, 121–158.

Hermann, J. (2002). Allanite: thorium and light rare earth element carrier in subducted crust. *Chemical Geology, 192*, 289–306.

Holland, T., & Blundy, J. (1994). Non ideal interactions in calcic amphiboles and their bearing on amphibole–plagioclase thermometry. *Contribution to Mineralogy and Petrology, 116*, 433–447.

Janots, E., Engi, M., Berger, A., Allaz, J., Schwarz, J. O., & Spandler, C. (2008). Prograde metamorphic sequence of REE minerals in pelitic rocks of the Central Alps, implications for allanite–monazite–xenotime phase relations from 250 to 610°C. *Journal of Metamorphic Geology, 26*, 509–526.

Kagami, H., Ulmer, P., Hansmann, W., Dietrich, V., & Steiger, R. H. (1991). Nd-Sr isotopic and geochemical characteristics of the southern Adamello (N Italy) intrusives: implications for crustal versus mantle origin. *Journal of Geophysical Research, 96*, B14331–B14346.

Kapferer, N. (2010). *The evolution of the surface of the Sesia–Lanzo Zone in Oligocene–Miocene times (Biella, NW Italy).* Dissertation, University of Bern, Bern, 169 pp.

Kapferer, N., Mercolli, I., & Berger, A. (2012a). The composition and evolution of an Oligocene regolith on top of the Sesia–Lanzo Zone (western Alps). *International Journal of Earth Science, 100*, 1115–1127.

Kapferer, N., Mercolli, I., Berger, A., Ovtcharova, M. & Fügenschuh, B. (2012b). Dating emplacement and evolution of the orogenic magmatism in the internal Western Alps: 2. The Biella Volcanic Suite. *Swiss Journal of Geoscience,105*. doi:10.1007/s00015-012-0092-6

Krummenacher, D., & Evernden, J. F. (1960). Détermination d'âge isotopique sur quelque roches des Alpes par la méthode K–Ar. *Schweizerische Mineralogische Petrographische Mitteilungen, 40*, 267–277.

Lustrino, M., Duggen, S., & Rosenberg, C. L. (2010). The central–western Mediterranean: anomalous igneous activity in an anomalous collisional tectonic setting. *Earth Science Review, 104*, 1–40.

Malaroda, R., Bertolami, G., Carraro, F., Friz, C., Govi, M., & Sacchi, R. (1966). Carta Geologica d'Italia, Foglio 43, "Biella". 1: 50,000. II ed., *Service Geologica Italia, Roma*.

Oberli, F., Meier, M., Berger, A., Rosenberg, C. L., & Gieré, R. (2004). ^{230}Th/^{238}U disequilibrium systematics in U–Th–Pb dating: precise accessory mineral chronology and melt evolution tracing in the Alpine Bergell intrusion. *Geochemica et Cosmochimica Acta, 68*, 2543–2560.

Owen, J. P. (2008). Geochemistry of lamprophyres from the western Alps, Italy: implications for the origin of an enriched isotopic component in the Italian mantle. *Contribution to Mineralogy and Petrology, 155*, 341–362.

Peccerillo, A., & Martinotti, G. (2006). The western Mediterranean lamproitic magmatism: origin and geodynamic significance. *Terra Nova, 18*, 109–117.

Pettke, T., Diamond, L. W., & Villa, I. M. (1999). Mesothermal gold veins and metamorphic devolatilization in the northwestern Alps: the temporal link. *Geology, 27*, 641–644.

Prelević, D., Foley, S. F., Romer, R. L., & Conticelli, S. (2008). Mediterranean tertiary lamproites: multicomponent melts in post-collisional geodynamics. *Geochimica and Cosmochimica Acta, 72*, 2125–2156.

Ricou, L. E., & Siddans, A. W. B. (1986). Collision tectonics in the western Alps. *Geological Society, London, Special Publications, 19*, 229–244.

Romer, R. L., Schärer, U., & Steck, A. (1996). Alpine and pre-Alpine magmatism in the root-zone of the western central Alps. *Contribution to Mineralogy and Petrology, 123*, 138–158.

Rosenberg, C. L. (2004). Shear zones and magma ascent: A model based on a review of the tertiary magmatism in the Alps. *Tectonics, 23*, TC3002.

Rosetti, P., Agangi, A., Castelli, D., Padoan, M., & Ruffini, R. (2007). The Oligocene Biella pluton (western Alps, Italy): new insights on the magmatic vs. hydrothermal activity in the Valsessera roof zone. *Periodico di Mineralogia, 76*, 223–240.

Schaltegger, U., Brack, P., Ovtcharova, M., Peytcheva, I., Schoene, B., Stracke, A., et al. (2009). Zircon and titanite recording 1.5 million years of magma accretion, crystallization and initial cooling in a composite pluton (southern Adamello batholith, northern Italy). *Earth and Planetary Science Letters, 286*, 208–218.

Schmid, S. M., Aebli, H. R., Heller, F., & Zingg, A. (1989). The role of the Periadriatic line in the tectonic evolution of the Alps. In D. Dietrich & M.P. Coward (Eds.), *Alpine tectonics* (Vol. 45, pp. 153–171). London: Geological Society of London Special Publication.

Schmidt, M. W. (1992). Amphibole composition in tonalite as a function of pressure: an experimental calibration of the Al-in-hornblende barometer. *Contribution to Mineralogy and Petrology, 110*, 304–310.

Stacey, J. S., & Kramers, J. D. (1975). Approximation of terrestrial lead isotope evolution by a two-stage model. *Earth and Planetary Science Letters, 26*, 207–221.

Stöckhert, B., & Gerya, T. V. (2005). Pre-collisional high pressure metamorphism and nappe tectonics at active continental margins: a numerical simulation. *Terra Nova, 17*, 102–110.

Thompson, A. B., Matile, L., & Ulmer, P. (2002). Some thermal constraints on crustal assimilation during fractionation of hydrous, mantle-derived magmas with examples from central Alpine Batholiths. *Journal of Petrology, 43*, 403–422.

Tommasini, S., Avanzinelli, R., & Conticelli, S. (2011). The Th/La and Sm/La conundrum of the Tethyan realm lamproites. *Earth and Planetary Science Letters, 301*, 469–478.

Van Marcke de Lumen, G., & Vander Auwera, J. (1990). Petrogenesis of Traversella diorite (Piemonte Italy): a major trace element and isotopic (O, Sr) model. *Lithos, 24*, 121–136.

Venturelli, G., Thorpe, R. S., Dal Piaz, G. V., Del Moro, A., & Potts, P. J. (1984). Petrogenesis of calc-alkaline, shoshonitic and associated ultrapotassic Oligocene volcanic rocks from the northwestern Alps, Italy. *Contribution to Mineralogy and Petrology, 86*, 209–220.

von Blanckenburg, F., Früh-Green, G., Diethelm, K., & Stille, P. (1992). Nd-, Sr-, O-isotopic and chemical evidence for a two-stage contamination history of mantle magma in the central-Alpine Bergell intrusion. *Contribution to Mineralogy and Petrology, 110*, 33–45.

von Blankenburg, F., Kagami, H., Deutsch, A., Oberli, F., Meier, M., Wiedenbeck, M., et al. (1998). The origin of Alpine plutons along the Periadriatic lineament. *Schweizerische Mineralogische Petrographische Mitteilungen, 78*, 57–68.

Watson, B. E., & Harrison, T. M. (1983). Zircon saturation revisted: temperature and composition effects in a variety of crustal magma types. *Earth and Planetary Science Letters, 64*, 295–304.

Winkler, W. (1983). Stratigraphie, Sedimentologie und sedimentpetrographie des Schlieren–Flysches (Zentralschweiz). *Beiträge zur Geologischen Karte der Schweiz, NF, 158*, 1–105.

Zanoni, D., Bado, L., Spalla, M. I., Zucali, M., & Gosso, G. (2008). Structural analysis of the northeastern margin of the tertiary intrusive stock of Biella (western Alps, Italy). *Bollotino della Societa Geologica Italiania, 127*, 125–140.

Zanoni, D., Spalla, M. I., & Gosso, G. (2010). Structure and PT estimates across late-collisional plutons: constraints on the exhumation of western Alpine continental HP units. *International Geology Review, 52*, 1244–1267.

Zingg, A., Hunziker, J., Frey, M., & Ahrendt, H. (1976). Age and degree of metamorphism of the Canavese zone of the sedimentary cover of the Sesia zone. *Schweizerische Mineralogische Petrographische Mitteilungen, 56*, 361–375.